Data Management and Domain Adjusting Strategies for Implementing Parallel SPH Method in JPUE Simulation

Zhixuan Cao, Abani Patra
Department of Mechanical and Aerospace Engineering
The University at Buffalo
Buffalo, New York 14260
Email: zhixuanc@buffalo.edu, abani@buffalo.edu

Matt Jones
Center for Computational Research
The University at Buffalo
Buffalo, New York 14260
Email: jonesm@buffalo.edu

Abstract

This paper presents a parallel implementation of smoothed particle hydrodynamics (SPH) method using the message passing interface (MPI) standard to simulate a turbulent jet or plume which is ejected from a nozzle into a uniform environment(JPUE). Background grid is used to reduce neighbors searching cost and decompose (redecompose) the domain. Space Filing Curve(SFC) based index is adopted to assign an unique identifier to each background grid. As simulation of JUPE requires adding of new particles during simulation, time-dependent SFC based indexes are assigned to particles to guarantee uniqueness of identifiers. Both particle and background grid are managed by hashtables which ensure quick and flexible accessing, adding and deleting of element. A SFC based three dimensional domain decomposition and a dynamic load balancing strategy are implemented to ensure good load balance. In addition, computational domain is adjusted during simulation to reduce computational cost. Numerical tests show that our code has acceptable strong scalability and good weak scalability. These strategies can be further applied to many other implementations of meshfree methods, especially those implementations that require irregular particle distributions, adding and deleting of particles and leverage adaptive background grids.

1. Introduction

SPH (smoothed particle hydrodynamics) is a meshless scheme, initially developed for astrophysical applications by Lucy [1] and Gingold and Monaghan [2]. Subsequently it was extended to computational fluid mechanics. A lot of research has appeared on parallellization of SPH in the last few years. Goozee [3] implemented a simple SPH code using MPI, OpenMP and BSP. Wenbo [4] presented a parallel SPH implementation on multi-core CPUs. Holmes [5] presented a simulation framework that enables distributed numerical computing in multi-core shared-memory environments. Dominguez [6] presented optimizations for both CPU and GPU parallelization of a SPH method. Ferrari [7] parallelized a 3D SPH code using the message passing interface (MPI) standard, together with a dynamic load balancing strategy to improve the computational efficiency of the scheme. Kumar et. al. [8] implemented a parallel Godunov SPH in simulation of granular flows. Crespo [9] used the GPUs to accelerate DualSPHysics by up to two orders of magnitude compared to the performance of the serial version.

However, most implementation of parallel SPH method presented to date are limited to standard SPH and benchmark problems like dam break, or relatively simple scenarios like breaking-waves, floodings etc. Work on more complicated problems, such as eruption of volcano plume which is essentially a mult-phase turbulent flow, ejection mixing process accompanied by microphysics phenomena like phase change of water, aggregation, reaction etc. is relatively rare. Prediction of such complicated phenomena with acceptable accuracy at given time window requires resolutions (very high particle counts) that cannot been accomplished without parallel computing. What's more, imposing of some types of boundary conditions (such as realistic wind field, eruption boundary condition) requires dynamically adding and removing of particles during simulation. This requires efficient and more flexible data management scheme. What we need to point out is that the benefit of flexible

data management strategies are not only limited to specific implementations of SPH. Actually, flexibility in data management are more critical for several advanced techniques of SPH, such as dynamic particle splitting techniques [10], [11], which will give greater resolution at the area of interest by splitting one large particle to several smaller ones. In this paper, we implement SPH to simulate a simplified version of complicated volcanic plume: the JPUE, and develop data management schemes for it.

Among existing CPU parallel SPH schemes, most of them focus on neighbors searching algorithm and dynamic load balancing. (eg. [7], [9]). Less attention has been paid to developing of more flexible data management schemes for more complicated problems. Fortunately, efficient and flexible data management strategies for high performance computing have been successfully implemented in mesh based methods (eg. [12] for adaptive hp FEM, and [13], [14] for FVM). Motivated by techniques developed for mesh based methods, we present a complete framwork for parallelizing SPH program with MPI standard model allowing more flexible and efficient data access in this paper.

Any implementation of SPH code requires efficient searching and updating of neighbors during simulation. Of the many choices possible for this we adopted a background grid which was proposed by Monaghan and Lattanzio [15] and is quite popular in parallel SPH. The background grid is also used for domain decomposition in SPH. We refer to the elements of background grid, namely squares for two dimension and cubics for three dimension, as buckets. As for the actual storage of data representing the physical quantities associated to each particle, different strategies have been adopted in existing implementations of SPH. In both SPHysics [6] and DualSPHysics [9], The physical quantities of each particle (position, velocity, density) are stored in arrays, and the particles (and the arrays with particle data) are reordered following the order of the cells. This has two advantages: 1) access pattern is more regular and more efficient, 2) it is ease to identify the particles that belong to a cell by using a range since the first particle of each cell is known. But adding, deleting and especially accessing of particles are cumbersome. Ferrari [7] adopted linked lists using pointers so that particles can be deleted or added during the simulation. Storage problems caused by fix-size arrays are thereby also eliminated. We define C++ classes which contains all data of particle and bucket. As for the management of data, we adopt a hash table to store pointers to particles and buckets,

which gives us not only flexibility of deleting and adding element, but also quicker access compared with linked list. Instead of using the "nature manner" to number particles, we adopt SFC based index to give each particle and background bucket an unique identifier – a strategy known to preserve some locality at minimal cost. The SFC based numbering strategy is further extended to include time step information so that particles added at the same position but different time will have different identifiers. As for domain decomposition, even though more complicated graph-based partition tools [16] might get higher quality decomposition, they requires much more effort in programming and computation. So we adopt an easy-programming scheme based on SFC [17].

To the best of the author's knowledge, no implementation of SPH has the feature of adjusting computational domain based on simulation needs. For JPUE simulation, such feature will greatly reduce computational cost by avoiding computing of uninfluenced fluid. This feature is accomplished by adding a scan function to monitor the outermost layer of the domain and turn ghost particles to real particles at proper time.

The data structure, particle and bucket indexing strategies, domain decomposition, dynamic load balancing method and domain adjusting strategies in this paper can be easily adopted by other implementations of any meshfree methods(include SPH). The flexibility of data accessing enables implementing of meshless methods for solving of more complicated problems and using of more advanced techniques.

2. Data Structure and Load Balance

SPH is a meshfree, Lagrangian method. The domain is discretized by particles and the position of each particle is updated at every time step. The physical laws (such as conservation laws of mass, momentum and energy) written in the form of partial differential equations need to be transformed into the Lagrangian particle formalism of SPH. Using a kernel function that provides the weighted estimate of the field variables in the neighborhood of a discrete point (particle), the integral equations are evaluated as sums over neighbor particles. Only particles located within support of kernel function will interact. Thus, physical properties (position, density, velocity, internal energy, pressure) are updated based on its neighbors. So a neighbor searching needs to be carried out before updating of physical properties. We use buckets which contain all
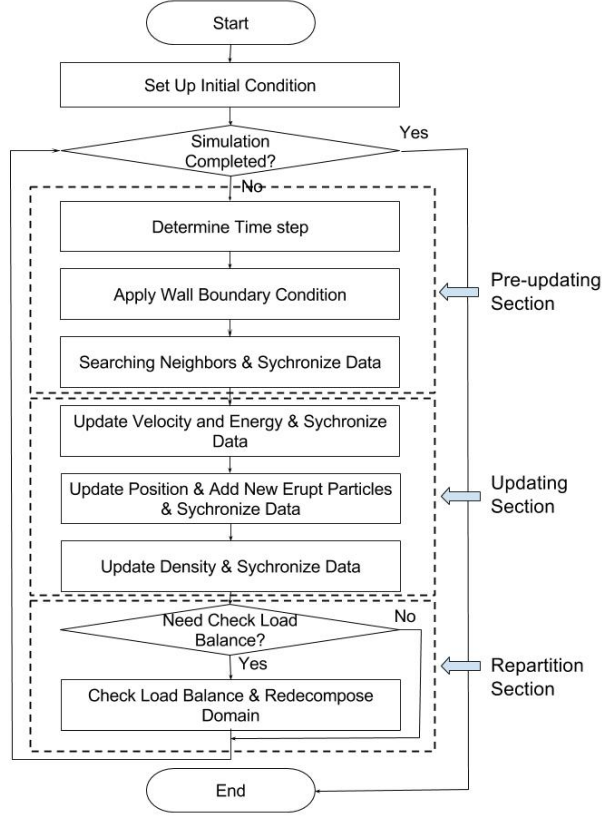
Figure 1. Basic work flow for SPH code

particles associated with a sub-domain and are kept fixed in time during the entire simulation, to reduce search cost (since search can now be restricted to only neighboring domains). Domain decomposition will be based on an SFC going through centroids of all buckets. A basic work flow of our SPH code is shown in figure 1.

Particles need to be added and(or) removed during simulation of JPUE problems. Wall boundary conditions in SPH can be imposed either by adding a force term or using ghost particles. We adopt the latter one in our simulation. As our computational domain will be adjusted during simulation, wall ghost particles need to be added during simulation. New particles also need to be added for the eruption boundary condition. We will describe in this section strategies which satisfy these requirements.

2.1. SFC based indexing

Our data structure starts from assigning each particle and bucket an identifier, we refer to it as key, which should be unique throughout simulation. The key for a bucket is determined by centroid coordinates of the

bucket while the key for a particle is determined by adding coordinates and adding time step of the particle. The map from coordinates to key is based on SFC.

The SFC [18] maps n-dimensional space to a one dimentional sequence. The standard procedure for obtainning SFC is:

- Scale coordinates into $[0, 1]^n$ based on maximum and minimum coordinates of the computational domain: $\mathbf{X}' \to \mathbf{X}$
- Compute $k_r = h_n(\mathbf{X})$. Where h_n is the map $h_n : [0, 1]^n \to [0, 1]$.
- Convert k_r to integer k by multiplying k_r with a very large number and removing decimal part.
- All keys are sorted to form a sequence which is SFC. The SFC represents a curve passing through all particles (or centroid of buckets).

Scheme for constructing the map h_n can be found in [19]. These keys denote a simple addressing/ordering scheme for the data and computations, i.e., a simple global index space for all the objects.

SFC-based indexing scheme can guarantee uniqueness of particle identifier only in simple scenarios when particles are added once while setting up initial condition. In some situations, new particles need to be added while simulation. For example, new particles need to be added at the bottom of the eject vent for JPUE simulation. To distinguish particles added at the "same place" (the small area, all points within which will be mapped to the same k.) at different time steps, we extend the SFC-based key to time-dependent SFC based key by including date of birth of particles into the key. The time-dependent SFC based key can be written as: $[k, t]$, where t is the time step. The map h_n will become:

$$h_n : [0, 1]^n \times \mathbf{T} \to [0, 1] \times \mathbf{N} \qquad (1)$$

Where $\mathbf{T} \subset [0, \infty)$ is the time step dimension, $\mathbf{N} = \{0, 1, 2, 3...\}$. To guarantee locality, sorting of particle keys is majorly based on k, that is to say, particle with smaller k always comes before particles with larger k. For these particles have the same k, ordering of them will depend on t. Figure 2.1 shows SFC ordering of buckets and particles in buckets. Several features of such indexing scheme are suitable for SPH:

- Guarantee uniqueness of keys.
- Key of each object is generated purely based on its own coordinates. When add new objects on different processes, key of each object can be generated fast and independently.
- Objects that locate closely in the Euclidian space will also be close to each other in the one dimensional SFC key space in the mean sense. Since
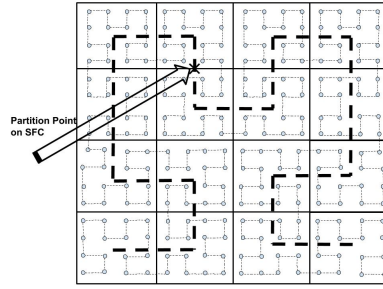
(a) SFCs passing all particles and buckets
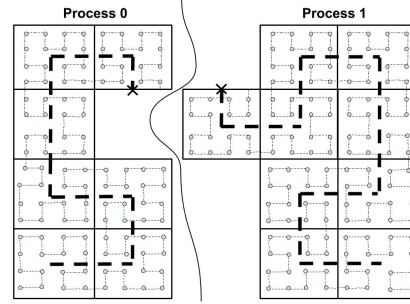
(b) Domain decomposition based on SFC of buckets

Figure 2. Spcace filling curve orderings of buckets and particles within the buckets

SPH particles only interact with its neighbors, geometric locality can be exploited for efficient storage and retrieval of bucket and particle data.

- This type of key effectively generates a global address space. Globality of key and conservation of locality make it easy to partition the sorted key sequence and obtain a decompositiion of the problem.

We need to emphasize here is that in theory motion of particles will destroy locality established based on initial coordinates of particles. However, as particles are moving fairly regularly in a JPUE, the locality of most of particles is largely conserved during simulation. We will revisit this question for more chaotic flows and design a re-numbering method which is computationally cheap, to restore the locality.

2.2. Data structure

2.2.1. Particle and bucket. The most basic data structure of SPH are particle, for problem description, and bucket, for neighbors searches and domain decomposition. Both are defined as classes in C++. Information that is contained in particle class can be categorized into six categories: ID(the key), affiliate(rank of the process that the particle belongs to), primitive variables (variables show up as unknowns in governing equations, e.g. density, velocity, energy), secondary variables (properties that can be computed from primitive variables, they are stored to avoid repeated computations eg. pressure, temperature), flags (indicators, such as indicator for ghost particle and real particles, indicator for particles of different phases) and neighbor information (it is a vector of particle keys in our application). Similarly, Information that is contained in a bucket class can also be categorized into different categories: ID(the key), affiliate(rank of the

process that the bucket belong to), domain information (maximum and minimum coordinates, boundary information), flags (indicators, such as indicator for guest and non-guest, indicator for active and inactive), neighbor information (keys of 27 neighbor buckets for three dimension and keys of 9 neighbor buckets for two dimension including its own key) and owned particles. Objects defined based on these two classes are then accessed through hash tables.

2.2.2. Hash table and hash conflict. As discussed at the beginning of this section, implementation of SPH in more realistic scenarios requires dynamic memory management and flexible data access. One of the fundamental data structures that satisfy such requirement is hash table. Another option is B-tree. We adopt hash table. An implementation of B-tree under a similar situation for mesh based methods can be found in other papers (eg. [20]).

Hash table, which is divided into slots, are array based data structure. Based on the key, the address-calculator(hashing) function determines in which slot the data should be stored. The hashing function maps from key to the slot index:

$$slot\,index = hash(key) \qquad (2)$$

The hash table has O(1) data access, adding and deleting properties when there is no conflict. How many conflicts will happen depends on both distribution of keys in the key space and size of the hash table. As the distribution of keys is determined by particles' initial locations (or centroids of buckets), the hash table size is under our control. We can use a very large hash table to minimize hash conflicts at the expense of sparse data distribution which will lead to high cache misses and low memory efficiency. Or alternately, we can use smaller hash
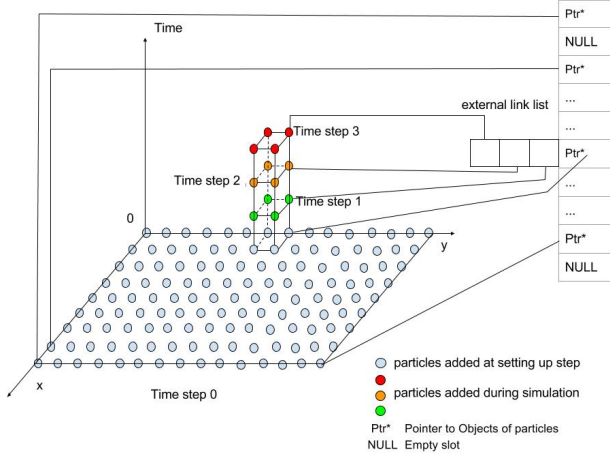
Figure 3. Non-uniform distribution of particles in the $[0,1]^n \times \mathbf{T}$ space due to adding of new particles at a small portion of the domain, pointer to these new particles will be stored in external link list.

table size to obtain high memory efficiency on the expense of having more hash conflicts. Patra et al. [20] did numerical experiments to examine the effect of the table size on the different data management operations.

One way to handle hash conflicts is by using an additional sorted vector attached to the hash table. When several keys hash to the same slot, a vector will be created. The vector is sorted based on keys so that a binary search can be used to find the correct position for adding, deleting or retrieving. Another option to handle hash conflicts is using an additional link list which is more flexible in memory allocation. The average time complexity of binary search is O(log n) while that for linear search based on link list is O(n). However, accessing efficiency of link list is much lower than array based data structure, especially when the link list becomes longer. Choosing of proper way to handle hash conflicts greatly depends on the problem itself. For the test problem in this paper, successively adding particles at the bottom of the eject vent will lead to hash conflicts of many particles, which implies a long link list. But considering the very long conflicts only occur on several slots among millions (see figure 3), we still choose the link list to handle hash conflicts. This decision was made based on numerical experiments.

2.2.3. Hash function. For time-independent keys, the hash function can be a simple function like:

$$Slot\,Index = \frac{Key - Min\,Key}{Max\,Key - Min\,Key} \times Hash\,Table\,Size \quad (3)$$

One natural way to hash time-dependent SFC based key $[k,t]$ is to convert the two elements in the key into one number taking k as the higher digit and t as the lower digit of the large number. However, for JPUE simulation, even though ghost particles for wall boundary condition and pressure boundary condition also need to be added during simulation, places for adding of these two types of ghost particles are previsouly empty area. Only ghost particles for eruption boundary condition will be successively added at the same place: bottom of the vent. That is to say, particles are distributed non-uniformly in the $[0,1]^n \times \mathbf{T}$ space as shown in figure 3. To avoid non-uniform, very sparse hash table and conserve locality of SFC, we only plug the first number, k, of the key, $[k,t]$, into the hashing function, equation (3).

2.3. Load balancing strategy

2.3.1. Weighted work load. Particles used in the test problem can be categorized into four types based on the particle-type-flag: real particle, wall ghost particle, pressure ghost particle and eruption ghost particle. Ghost particles are for imposing of corresponding boundary conditions (see figure 5). As different types of particles involve different amount of computational work, shown by table 2 and table 1, we assign different work load weight for different types of particles based on profilling data. Instead of simply using number of contained particles as work load for bucket, work load of each bucket is determined by summing up work load weight of all particles within the bucket. The SFC sequence passing through centroids of all buckets now becomes a weighted sequence. Domain decomposition is conducted based on the weighted SFC of buckets.

2.3.2. Domain decomposition and dynamic load balancing. Figure 2 shows how domain is decomposed based on partition of SFC of buckets. The particles are automatically split into several groups along with buckets that contain them. As SFC of buckets is a curve in the three dimensional space, partition of this curve will automatically lead to 3D domain decomposition. A 2D domain decomposition based on SFC of footprint buckets projected by three dimensional buckets was adopted by Kumar et al [8]. A comparison of the

Table 1. Computational Cost Per Particle for Different Steps

Step	Cost (ms)	Abbreviation
neighbor search	0.41	NS
update momentum and energy	0.70	UPME
update density	0.42	UPD
update position	0.02	UPP
velocity filtering	0.43	VF
apply wall bc	0.75	WBC

Table 2. Computational Work Load for Each Type of Particle

Particles	NS	UPME	UPD	UPP	VF	WBC	Total
Real	Yes	Yes	Yes	Yes	Yes	No	2.00
wall	No	No	No	No	No	Yes	0.75
eruption	No	No	No	Yes	No	No	0.02
pressure	No	No	No	No	No	No	0.00

Figure 4. Work flow that enables domain adjusting feature

scalability of these two schemes (see figure 8) confirms that 3D domain decomposition is a better choice when processes number is larger. Movement of particles, adding of new particles, adjusting of domain will lead to important load imbalance between processes. To handle this, computational load is monitored at a given interval (The interval is optimized based on numerical experiments). And repartitioning is carried out when load imbalance is larger than a given tolerance.

As some of the neighbor particles reside in other partitions. A set of particles and buckets are used to synchronize data across partitions. To minimize communications, data is synchronized only where needed, using non-blocking MPI communications.

3. Adjusting of Domain During Simulation

As a Lagrangian method, SPH is able to automatically define and adjust its computational domain as the position of the discretization points are updated at every time step. The collective support of the SPH particles defines the computational domain. However, for JPUE simulation (and many similar/related phenomena), where some fluid ejects into stationary fluid and gets mixed, the domain-adjusting feature of SPH cannot be taken advantage of as all of the stationary fluid must be represented. A lot of CPU time will be spent on computing associated with these stationary particles. If simulating of stationary particles can be avoided, the computational cost will be reduced greatly. We propose a simple strategy to add such feature in our code with low computational cost. We add a scan function to monitor
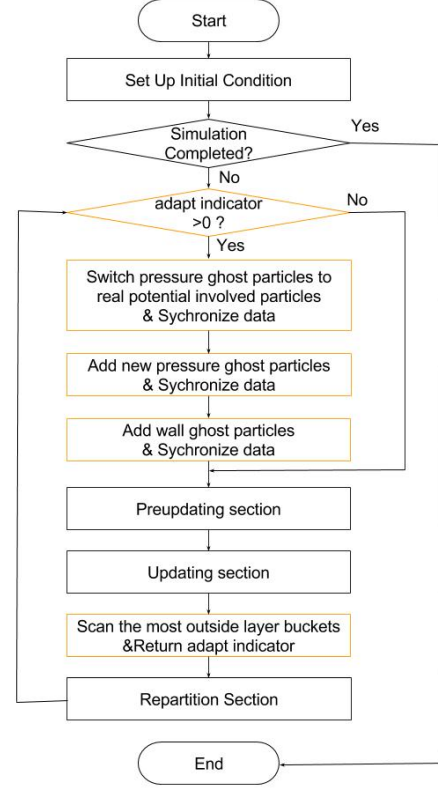
the most outside layer of the domain. When the ejected fluid reaches the boundary of the current domain, ghost particles (for pressure boundary condition) will be turn to real particles and then add new ghost particles for pressure boundary condition. The original work flow (see figure 1) is modified to enable such a feature (see figure 4).

This is implemented by using a involved-flag, in the particle class. Particles are categorized into three groups based on the value of the involved-flag: involved (involved-flag=2), potentially involved (involved-flag=1), and not involved (involved-flag=0). The involved particles are particles that have already been affected by the mixing. The potentially involved particles are particles that have not been involved in mixing but are adjacent to involved particles and will thus be be involved in the near future. All communication and computation associated with uninvolved particles can be ignored. That is to say, only potential involved and involved particles need to be simulated. As simulation progresses, the ejected fluid will reach larger area and more and more particles will be influenced. When originally

stationary air is influenced by erupted material, the mass fraction of the erupted material will increase from zero to a positive value. So we can determine whether a particle is involved or not based on whether the mass fraction of that particle is larger than a given threshold (10^{-5} in our simulation). Other physical properties, like velocity, can also serve as alternative "swich criteria".

A similar scheme can also be deployed for buckets resulting in a categorization of buckets. The additional complexity here is that potentially involved ghost particles must also be accounted for. This domain adjusting process is shown in figure 5. The work flow with domain adjusting is in figure 4

4. Numerical Test

Our target here is to develop data management and parallelization strategies for more complicated implementations of SPH which demand quick and flexible data access, deletion and addition. Thus, the test problem used should have such requirements. Simulations of a volcanic eruption, which is essentially a mutiphase, turbulent, ejection mixing flow accompanied with microphysics processes will place these demands on the framework. Thus, we adopt a two phase volcanic plume model [21] as our test problem. In this model, one phase is air while another phase is ejected material.

4.1. Governing equations [21] and boundary conditions

Based on Navier-Stokes equations and several simplifications, the governing equations in Eulerian form are:

$$\frac{\partial \rho}{\partial t} + \nabla \cdot (\rho \mathbf{v}) = 0 \qquad (4)$$

$$\frac{\partial \rho \xi}{\partial t} + \nabla \cdot (\rho \xi \mathbf{v}) = 0 \qquad (5)$$

$$\frac{\partial \rho \mathbf{v}}{\partial t} + \nabla \cdot (\rho \mathbf{v v} + p \mathbf{I}) = \rho \mathbf{g} \qquad (6)$$

$$\frac{\partial \rho E}{\partial t} + \nabla \cdot [(\rho E + p) \mathbf{v}] = \rho \mathbf{g} \cdot \mathbf{v} \qquad (7)$$

ξ is the mass fraction of ejected material. $E = e + K$ is total energy which is summation of kinetic energy K and internal energy e. An additional equation is required to close the system. In this model, the equation for closing the system is an EOS:

$$p = (\gamma_m - 1)\rho e \qquad (8)$$

Where

$$\gamma_m = R_m / C_{vm} + 1 \qquad (9)$$

$$Rm = n_g R_g + n_a R_a \qquad (10)$$

$$C_{vm} = n_s C_{vs} + n_g C_{vg} + n_a C_{va} \qquad (11)$$

$$n_a = 1 - \xi \qquad (12)$$

$$n_g = \xi n_{g0} \qquad (13)$$

$$n_s = \xi - n_g \qquad (14)$$

Where, C_v is specific heat with constant volume, n is mass fraction, R is gas constant. The subscript m represents mixture of ejected material and air, s is solid portion in ejected material, g is gas portion in the ejected material and a is air.

In current model the initial domain is a 3D box. The boundaries are categorized into eruption vent (a circle area at the center of the bottom), wall boundary (box bottom), pressure boundary (Other faces of the box). At the vent, T, $\mathbf{v} = \{0, 0, 150\}^T$, $p = 1.01 \times 10^5 Pa$, $n_{g0} = 0.05$ and mass discharge rate $\dot{M}$ is given. The radius of vent is determined from ρ, $\dot{M}$ and $\mathbf{v}$. Velocity is zero for non-slip wall boundary. We assume the boundary to be adiabatic and the heat flux is zero on the boundary. The pressure of the surrounding atmosphere is specified on pressure boundaries. Except for the pressure, density, velocity, and energy will depend on the solution. We adpot ghost particles to impose these different type of boundary conditions (see figure 5).

4.2. Discretized governing equations with SPH

There are several review papers [22], [23], [24], [25], [26] which provide a pretty comprehensive descriptions of SPH. These may be consulted for additional detail.The discretized governing equations with SPH are:

$$< \rho_a^a > = \sum m_b w_{ab}(h_a) \qquad (15)$$

$$< \rho_i^{sg} > = \sum_j m_j w_{ij}(h_i) \qquad (16)$$

$$< \frac{d\mathbf{v}_\alpha}{dt} > = -\sum_b [m_b (\frac{p_b}{\rho_b^2} + \frac{p_\alpha}{\rho_\alpha^2} + \Pi_{\alpha b})$$
$$\nabla_\alpha w_{\alpha b}(h_\alpha)] - \sum_j [m_j (\frac{p_j}{\rho_j^2} \qquad (17)$$
$$+ \frac{p_\alpha}{\rho_\alpha^2} + \Pi_{\alpha j}) \nabla_\alpha w_{\alpha j}(h_\alpha)] + \mathbf{g}$$

$$< \frac{de_\alpha}{dt} > = 0.5 \sum_b [m_b \mathbf{v}_{\alpha b} (\frac{p_b}{\rho_b^2} + \frac{p_\alpha}{\rho_\alpha^2} + \Pi_{\alpha b})$$
$$\nabla_\alpha w_{\alpha b}(h_\alpha)] + 0.5 \sum_j [m_j \mathbf{v}_{\alpha b} (\frac{p_j}{\rho_j^2} \qquad (18)$$
$$+ \frac{p_\alpha}{\rho_\alpha^2} + \Pi_{\alpha j}) \nabla_\alpha w_{\alpha j}(h_\alpha)]$$

(a) Computational domain at $t = t0$ (b) Computational domain at $t = t0 + \delta t$
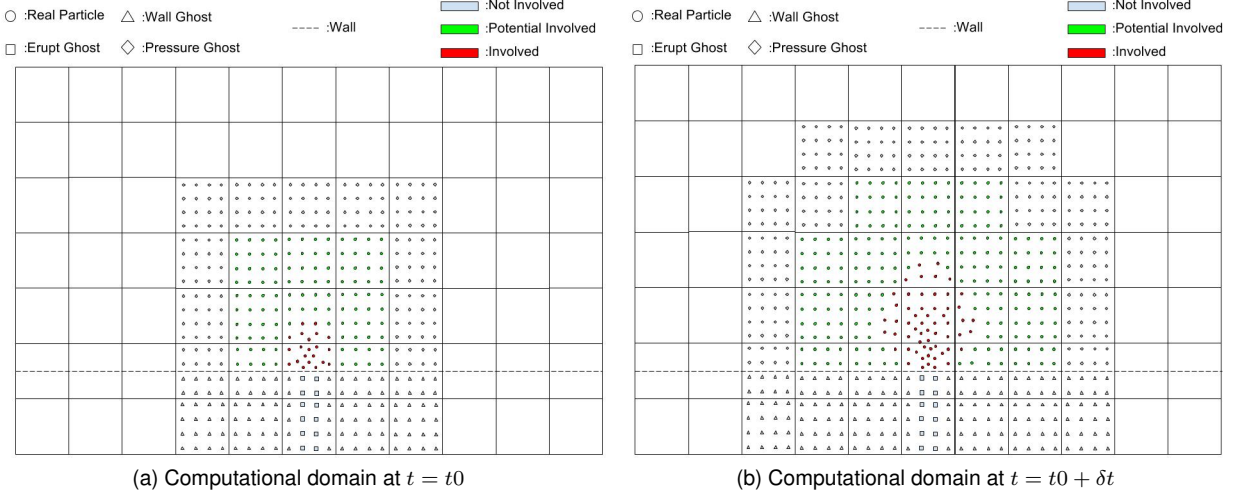
Figure 5. Adjusting the domain based on involved-flag of particles

Where ρ_a^a is density of phase 1 (air). ρ_i^{sg} is density of phase 2 (erupted material). $\rho = \rho^a + \rho^{sg}$ is density of mixture of phase 1 and phase 2.

$$\mathbf{v}_{\alpha b} = \mathbf{v}_\alpha - \mathbf{v}_b \qquad (19)$$

$$\mathbf{v}_{\alpha j} = \mathbf{v}_\alpha - \mathbf{v}_j \qquad (20)$$

$w_{ab}(h_a) = w(\mathbf{r}_a - \mathbf{r}_b, h_a)$ is smoothing kernel. Π is artificial viscosity term [22]. Index a, b is for phase 1. Index i, j is for phase 2. Index α, β can be index of either phase 1 or phase 2. The position of each particle is updated according to the following equation.

$$\frac{d\mathbf{r}_a}{dt} = \mathbf{v} \qquad (21)$$

Free surface flows are inherently turbulent. We adopt $SPH - \varepsilon$ method developed by Monaghan [27] to capture turbulence in the plume. This will result in a filtered velocity for position updates and additional turbulent terms in momentum and energy equation.

4.3. Solver performance

Experiments have been carried out on the computational cluster of Center for Computational Research (CCR) at Buffalo. Two types of processors – 8 core L5630 running at 2.13GHz clock rate with 3GB memory per core on a Mellanox network and 12 core E5645 running at 2.40GHz clock rate with 4GB memory per core on a Q-Logic network. Each node comprised of two sockets with two of these processors. Memory and level 3 cache are shared on each node. An important caveat in interpreting these results is that they were obtained in settings where the processors
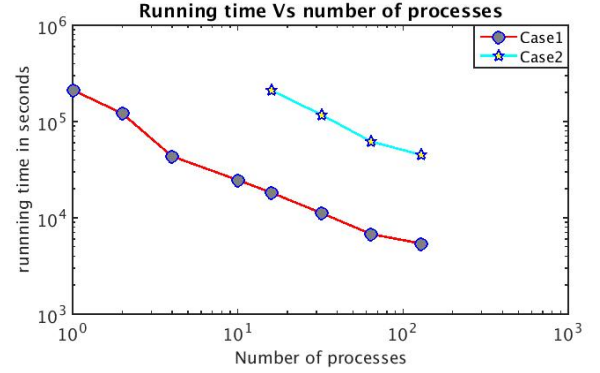

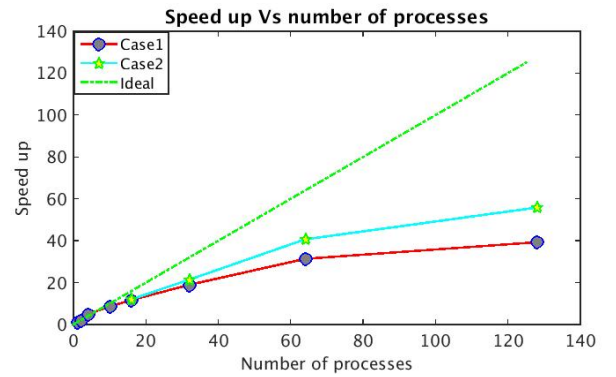Figure 6. Execution time of test case 1 and test case 2

Figure 7. Influence of total work load on strong scalability

were obtained under normal scheduling (hence readily available) wherein the nodes may be shared with other
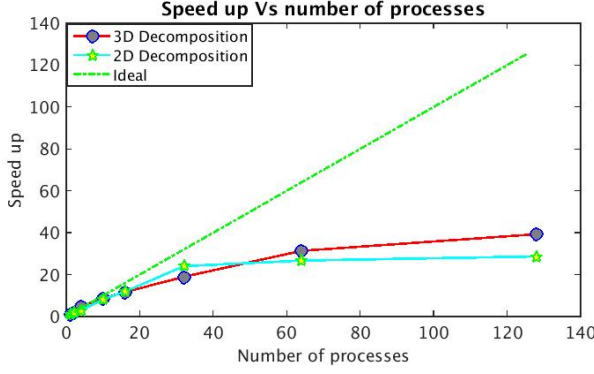
Figure 8. Strong scalability of 3D domain decomposition and 2D domain decomposition
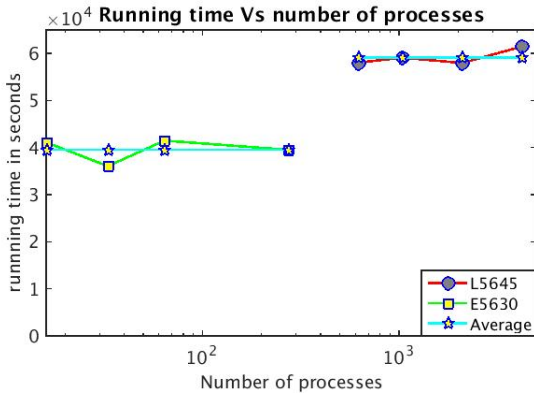

Figure 9. Weak scalability test results

users. Thus our results may suffer from contention for memory, CPU-memory bandwidth and network access. As of this writing, we are waiting for exclusive access which will undoubtedly provide better results. On the other hand, these results are representative of what will be available during production use. The initial domain is $[-4800m, 4800m] \times [-4800m, 4800m] \times [0m, 6000m]$, with smoothing length (we set initial intervals between particles equal to smoothing length) equals to 200m and 100m respectively for test case1 and test case2, respectively. The computational work load of test case 2 is 8 times of that of the test case 1. The simulations run for 20s physical time. Wall clock time and speed up are shown in figure 6 and 7. Linear speed up is observed when number of processes is smaller than 16. Test case2 shows better speed up than test case1 which implies that the overhead of strong scalability can be increased by increasing total amount of work load. We also compared the performance of 2D domain decomposition and 3D domain decomposition. As shown by figure 8, 2D

domain decomposition shows a little bit better speed up than 3D domain decomposition for 32 processes. This can be explained by the fact that 2D domain decomposition can get more regular subdomain and as a results, need less communication. When number of processes increase, it becomes harder for 2D decomposition to balance workload, that is why 3D domain decomposition has better speed up for processes number equals to 64 and 128. The weak scalability test is conducted with the same initial domain and various smoothing length. Each simulation runs for 400 loops. The average number of real particles of each process keep constant at 25900. As shown in figure 9, simulation time are almost constant with some minor fluctutations around the average value. These fluctuations are due to sharing nodes with other users. In addition, difference in simulation time for different processors are obvious. For the test problem in this paper, the volcanic plume will finally reach to a region of $[-10km\ 10km] \times [-10km\ 10km] \times [0km\ 20km]$ after around 300 seconds of eruption. When numerical simulation goes up to 90 seconds, the plume is still within a region of $[-3km\ 3km] \times [-3km\ 3km] \times [0km\ 6km]$. This implies that adjusting of domain can avoid computing large number of uninfluenced air particles, especially for the beginning stage of simulation. Numercial test shows that simulation time of the test problem is reduce to $\frac{1}{4}$ of original simulation time when we adopt the domain adjusting strategy in our code.

5. Conclusion

We developed data management strategies for parallel implementation of SPH method using MPI standard to simulate complicated problems, such as JUPE, which requires flexible and fast data retrievalling, adding and deleting. Neighbors searching and domain decomposition is based on background grid which overlaps the domain and keep stationary during simulation. SFC based index scheme, which provides a global numberring methodology which is purely coordinates dependent, is adopted to give each bucket an unique identifier. A time dependent key which is also based on SFC is used as identifier for particle. Hashtables with external link list are adopted for accessing particles and buckets data. Based on weighted particle work load, a dynamic load balance strategy is developed by checking load balance and redecomposing the domain at an optimize interval. The performance of the code was further improved to several times faster by adjusting computational domain according to progress of simulation. Scalability tests on

our code shew acceptable strong scalability and good weak scalability. 3D domain decomposition provided better strong scalability than 2D domain decomposition when number of processes is larger.

Acknowledgments

References

[1] L. B. Lucy, "A numerical approach to the testing of the fission hypothesis," *The astronomical journal*, vol. 82, pp. 1013–1024, 1977.

[2] R. A. Gingold and J. J. Monaghan, "Smoothed particle hydrodynamics: theory and application to non-spherical stars," *Monthly notices of the royal astronomical society*, vol. 181, no. 3, pp. 375–389, 1977.

[3] R. J. Goozée and P. A. Jacobs, "Distributed and shared memory parallelism with a smoothed particle hydrodynamics code," *ANZIAM Journal*, vol. 44, pp. 202–228, 2003.

[4] C. Wenbo, Y. Yao, and Y. Zhang, "Performance analysis of parallel smoothed particle hydrodynamics on multicore cpus," in *Cloud Computing and Internet of Things (CCIOT), 2014 International Conference on*. IEEE, 2014, pp. 85–90.

[5] D. W. Holmes, J. R. Williams, and P. Tilke, "A framework for parallel computational physics algorithms on multi-core: Sph in parallel," *Advances in Engineering Software*, vol. 42, no. 11, pp. 999–1008, 2011.

[6] J. M. Domínguez, A. J. Crespo, and M. Gómez-Gesteira, "Optimization strategies for parallel cpu and gpu implementations of a meshfree particle method," *arXiv preprint arXiv:1110.3711*, 2011.

[7] A. Ferrari, M. Dumbser, E. F. Toro, and A. Armanini, "A new 3d parallel sph scheme for free surface flows," *Computers & Fluids*, vol. 38, no. 6, pp. 1203–1217, 2009.

[8] D. Kumar, A. K. Patra, E. B. Pitman, and H. Chi, "Parallel godunov smoothed particle hydrodynamics (sph) with improved treatment of boundary conditions and an application to granular flows," *Computer Physics Communications*, vol. 184, no. 10, pp. 2277–2286, 2013.

[9] A. Crespo, J. Domínguez, B. Rogers, M. Gómez-Gesteira, S. Longshaw, R. Canelas, R. Vacondio, A. Barreiro, and O. García-Feal, "Dualsphysics: Open-source parallel cfd solver based on smoothed particle hydrodynamics (sph)," *Computer Physics Communications*, vol. 187, pp. 204–216, 2015.

[10] R. Vacondio, B. Rogers, and P. Stansby, "Accurate particle splitting for smoothed particle hydrodynamics in shallow water with shock capturing," *International Journal for Numerical Methods in Fluids*, vol. 69, no. 8, pp. 1377–1410, 2012.

[11] J. Feldman and J. Bonet, "Dynamic refinement and boundary contact forces in sph with applications in fluid flow problems," *International Journal for Numerical Methods in Engineering*, vol. 72, no. 3, pp. 295–324, 2007.

[12] A. Laszloffy, J. Long, and A. K. Patra, "Simple data management, scheduling and solution strategies for managing the irregularities in parallel adaptive hp finite element simulations," *Parallel Computing*, vol. 26, no. 13, pp. 1765–1788, 2000.

[13] E. B. Pitman, C. C. Nichita, A. Patra, A. Bauer, M. Sheridan, and M. Bursik, "Computing granular avalanches and landslides," *Physics of Fluids (1994-present)*, vol. 15, no. 12, pp. 3638–3646, 2003.

[14] A. K. Patra, A. Bauer, C. Nichita, E. B. Pitman, M. Sheridan, M. Bursik, B. Rupp, A. Webber, A. Stinton, L. Namikawa *et al.*, "Parallel adaptive numerical simulation of dry avalanches over natural terrain," *Journal of Volcanology and Geothermal Research*, vol. 139, no. 1, pp. 1–21, 2005.

[15] J. J. Monaghan and J. C. Lattanzio, "A refined particle method for astrophysical problems," *Astronomy and astrophysics*, vol. 149, pp. 135–143, 1985.

[16] R. Biswas and L. Oliker, "Experiments with repartitioning and load balancing adaptive meshes," in *Grid Generation and Adaptive Algorithms*. Springer, 1999, pp. 89–111.

[17] A. Patra and D. Kim, "Efficient mesh partitioning for adaptive hp finite element meshes," in *In International Conference on Domain Decomposition Methods*. Citeseer, 1999.

[18] H. Sagan, *Space-filling curves*. Springer Science & Business Media, 2012.

[19] A. Patra and J. T. Oden, "Problem decomposition for adaptive hp finite element methods," *Computing Systems in Engineering*, vol. 6, no. 2, pp. 97–109, 1995.

[20] A. Patra, A. Laszloffy, and J. Long, "Data structures and load balancing for parallel adaptive hp finite-element methods," *Computers & Mathematics with Applications*, vol. 46, no. 1, pp. 105–123, 2003.

[21] Y. J. Suzuki, T. Koyaguchi, M. Ogawa, and I. Hachisu, "A numerical study of turbulent mixing in eruption clouds using a three-dimensional fluid dynamics model," *Journal of Geophysical Research: Solid Earth (1978–2012)*, vol. 110, no. B8, 2005.

[22] J. J. Monaghan, "Smoothed particle hydrodynamics," *Annual review of astronomy and astrophysics*, vol. 30, pp. 543–574, 1992.

[23] J. Monaghan, "Smoothed particle hydrodynamics," *Reports on progress in physics*, vol. 68, no. 8, p. 1703, 2005.

[24] D. J. Price, "Smoothed particle hydrodynamics and magnetohydrodynamics," *Journal of Computational Physics*, vol. 231, no. 3, pp. 759–794, 2012.

[25] S. Rosswog, "Astrophysical smooth particle hydrodynamics," *New Astronomy Reviews*, vol. 53, no. 4, pp. 78–104, 2009.

[26] J. Monaghan, "Smoothed particle hydrodynamics and its diverse applications," *Annual Review of Fluid Mechanics*, vol. 44, pp. 323–346, 2012.

[27] J. J. Monaghan, "A turbulence model for smoothed particle hydrodynamics," *European Journal of Mechanics-B/Fluids*, vol. 30, no. 4, pp. 360–370, 2011.